JAAS

TECHNICAL NOTE

View Article Online
View Journal | View Issue

Cite this: *J. Anal. At. Spectrom.*, 2015, **30**, 994

In situ simultaneous measurement of Rb–Sr/Sm–Nd or Sm–Nd/Lu–Hf isotopes in natural minerals using laser ablation multi-collector ICP-MS†

Chao Huang, Yue-Heng Yang,* Jin-Hui Yang and Lie-Wen Xie

Received 20th November 2014
Accepted 23rd February 2015

DOI: 10.1039/c4ja00449c

www.rsc.org/jaas

This study presents a combined methodology of simultaneously measuring Rb–Sr/Sm–Nd or Sm–Nd/Lu–Hf isotopes in natural minerals by a means of two multiple collector inductively coupled plasma mass spectrometers (MC-ICP-MSs) connected to a 193 nm excimer laser ablation system. The ablated materials carried out of the HelEx cell by helium gas are split into two gas streams with different proportions into the Neptune for Sr (or Nd) analyses and Neptune Plus for Nd (or Hf) analyses. Experiments show that the different proportions of the ablated material for the Neptune and Neptune Plus MC-ICP-MS (3 : 7, 5 : 5 and 7 : 3) do not show any significant bias for the Sr–Nd isotopes on apatite and loparite within analytical uncertainties. Therefore, we conclude that this technique is suitable to simultaneously measure Rb–Sr and Sm–Nd or Sm–Nd and Lu–Hf isotopes in natural minerals, such as apatite, perovskite, loparite and eudialyte for Sr–Nd isotopes as well as eudialyte and zirconolite for Nd–Hf isotopes.

1. Introduction

Rb–Sr, Sm–Nd and Lu–Hf isotopes are not only important tracers in geochemistry and geochronology, but also important tools for deciphering petrogenesis and crust–mantle evolution in our planet.[1–8] Recently, the rapid development in multi-collector inductively coupled plasma mass spectrometry combined with laser ablation technique (LA-MC-ICP-MS) makes it possible to rapidly determine *in situ* Sr or Nd or Hf isotopes in minerals containing these isotopes (*e.g.*, apatite, perovskite, loparite, zircon, eudialyte and zirconolite). This technique is a more powerful tool for constraining geological processes than whole rock analysis.[6–13] The different elements in geology used for radiogenic isotope studies vary significantly depending on their chemical and physical properties; therefore, the sensitivity of the different isotope systems will vary depending on particular petrological processes. A good example is the difference in the Sm–Nd system, in which both the elements share similar chemical and physical characteristics, and the Rb–Sr system, in which both the elements are strongly fractionated. Therefore, a combined study of two or more isotopic systems can more accurately and precisely constrain the petrogenesis and crust–mantle evolution on Earth.

The routine analytical technique for *in situ* Sr, Nd or Hf isotopes can only measure one element at a time. Therefore, to measure Sr–Nd–Hf isotopes in natural minerals, three different analyses must be carried out. In that case, it will not be an *in situ* simultaneous determination of Sr–Nd–Hf isotopes because the information provided is not obtained from the same volume of material. The synthetic analysis of the multiple isotopes of the same volume of material is the main trend for the *in situ* Sr, Nd and Hf isotopic analysis in the near future.[14–17] For example, the first simultaneous measurements of U–Pb/Lu–Hf isotopes, and trace elements in zircon reference materials were reported by Yuan *et al.*[15] The materials were measured using a quadrupole ICP-MS (Elan6100 DRC) and a MC-ICP-MS (Nu Plasma HR), and the results agree with the reference values. Xie *et al.*[14] also performed in the situ simultaneous measurements of U–Pb/Lu–Hf isotopes, and trace elements in zircon and baddeleyite reference materials using a quadrupole ICP-MS (Agilent 7500a) and a MC-ICP-MS (Neptune). The results also agree with the reference values. As in our study, the authors did not find any evidence of increased elemental fractionation when the aerosol was split in different proportions. Tollstrup *et al.*[16] used a HR-ICP-MS (ELEMENT XR) and a MC-ICP-MS (NEPTUNE Plus) to carry out simultaneous measurements of U–Pb ages and Lu–Hf isotopes in zircon. In that study, it was found that the U–Pb ages of various reference materials were accurate within 0.3–2.5% (2σ) range compared to the TIMS value, and $^{176}Hf/^{177}Hf$ ratios were accurate within 0.28–0.73% (2σ) range relative to the solution MC-ICP-MS values, which demonstrates the potential of the simultaneous measurement of both isotope ratios and trace elements.

State Key Laboratory of Lithospheric Evolution, Institute of Geology and Geophysics, Chinese Academy of Sciences, P. B. 9825, Beijing, 100029, P. R. China. E-mail: yangyueheng@mail.iggcas.ac.cn; Fax: +86-010-62010846; Tel: +86-010-82998599

† Electronic supplementary information (ESI) available. See DOI: 10.1039/c4ja00449c

In this study, we developed a technique for the simultaneous determination of Rb–Sr/Sm–Nd or Sm–Nd/Lu–Hf isotopes during the *in situ* laser ablation using two MC-ICP-MSs (Neptune and Neptune Plus) and an excimer ArF laser-ablation system (Analyte G2) hosted at the Institute of Geology and Geophysics, Chinese Academy of Sciences. This method is validated by the simultaneous measurements of Sr–Nd isotopes in apatite, perovskite, loparite and eudialyte or Nd–Hf isotopes in eudialyte and zirconolite. The results are consistent with previously reported values, which indicate the reliability and robustness of our analytical protocol.

2. Experimental methodology

2.1. Instrumentation

All the accessory minerals investigated in this study were analyzed at the State Key Laboratory of Lithospheric Evolution, the Institute of Geology and Geophysics, Chinese Academy of Sciences, Beijing. The analyte G2 laser ablation system (Photon Machines, USA) is powered by an ATLex 300si 193 nm excimer laser. It has full (0–100%) energy attenuation, beam homogenization optics and a maximum energy density of 15 J cm^{-2}. The sizes of the laser spot vary between 1–150 μm and include circular, square, cross and slit-shaped spots. Pulse width is less than 4 ns, and frequency varies from 1 to 300 Hz. It is equipped with an ANU HelEx 2-volume cell having a 100 cm square useful sample area, which allows for the efficient transport of sample into the mass spectrometer. This cell minimizes the washout times and enables the sequential, rapid and reliable analysis of multiple ablation sites. A laser repetition rate of 12 Hz was used in this study, and the spot sizes ranged from 40 μm to 130 μm, depending on the Sr, Nd and Hf concentration in the samples. Helium was used as the carrier gas within the ablation cell.

Sr, Nd and Hf isotopic analyses were carried out by the Thermo Fisher Scientific Neptune and Neptune Plus MC-ICP-MSs (Bremen, Germany) combined with the analyte G2, as shown in Fig. 1. A detailed description of the instruments can be found elsewhere.[10,14] The Sr, Nd and Hf isotopic data were acquired by a static multi-collection in low-resolution mode using nine Faraday collectors. The detailed parameters are summarized in Tables 1 and 2.

The 193 nm laser beam is generated from an ATLex 300si 193 nm excimer laser, homogenized by optics, modulated to the right spot size by the aperture and finally reaching the surface of the samples. The ablated sample aerosol carried out of the HelEx cell by helium is split into two portions using a Y-shaped connector; one is transported to the Neptune and the other to the Neptune Plus. Both of them can be adjusted by two gas flow controllers between the Y-shaped connector and the gas mixers to achieve different gas flow ratios and ensure sufficient signals for Sr–Nd or Nd–Hf isotopic analyses. The sample aerosol of the two gas streams was mixed with Ar sample gas from two MC-ICP-MSs prior to introducing the aerosol into the plasma.

2.2. Data reduction

The *in situ* Sr, Nd and Hf isotopic measurements using LA-MC-ICP-MS were described in detail,[5,10,18] therefore, herein, we only provide a brief description of the data reduction procedure. For Sr isotopic analysis, the potential isobaric interferences were taken into account for Kr, Yb, Er and Rb. The interference of ^{84}Kr and ^{86}Kr on ^{84}Sr and ^{86}Sr, respectively, was removed using the 40 s Kr gas baseline measurement. The interference of Er and Yb on Sr masses was monitored using the isotopic abundances of Er and Yb.[19] The natural ratio of $^{85}Rb/^{87}Rb$ was used to correct the isobaric interference of ^{87}Rb on ^{87}Sr by the

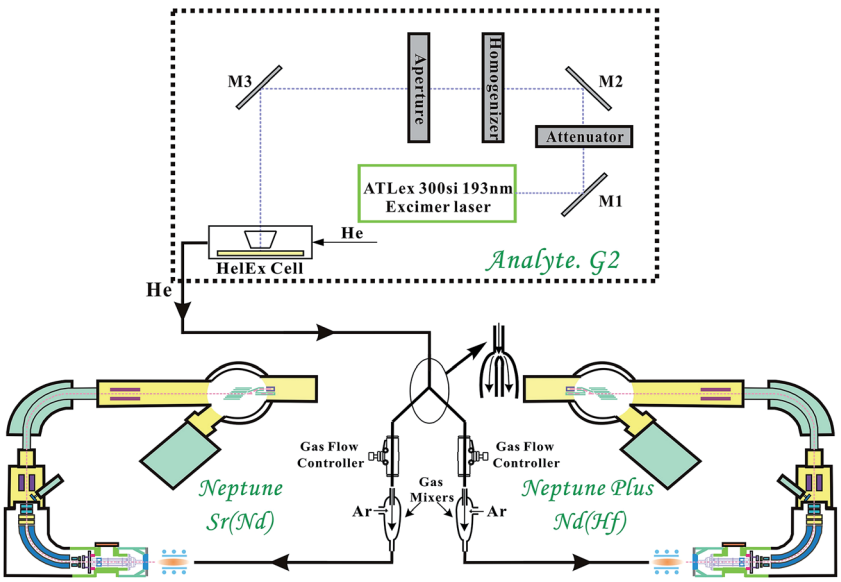

Fig. 1 Schematic illustration of the analytical protocol for the simultaneous *in situ* Sr–Nd or Nd–Hf isotopic analyses of accessory minerals. The experimental setup of the analyte G2 laser ablation, and the simultaneous determination of Sr(Nd) isotope on the Neptune MC-ICP-MS and Nd(Hf) isotope on the Neptune Plus MC-ICP-MS.

Table 1 Typical instrumental operating conditions and data acquisition parameters

Mass spectrometry parameters		
Instrument	Neptune	Neptune Plus
RF forward power	1340 W	1280 W
Reflect RF power	<−3 W	<−3 W
Cool gas	16 L min^{-1}	16 L min^{-1}
Auxiliary gas	0.8 L min^{-1}	0.8 L min^{-1}
Sample gas	1.2 L min^{-1}	0.8 L min^{-1}
Sample cones	Sample cone Ni	Sample cone Ni
Skimmer cones	High performance	High performance
Integration time	0.131 s for each cycle; 1 block; 200 cycles	0.131 s for each cycle; 1 block; 200 cycles
Isotopes	Sr(Nd)	Nd(Hf)
Laser ablation system (Analyte G2)		
Laser system		ATLex 300si, ArF excimer, wavelength UV 193 nm
Energy density		3.18 J cm^{-2}
Spot size		130 μm for MAD, 110 μm for AP1 and LV-1, 85 μm for AFK and ZrkA, 65 μm for NW-1, 50 μm for SDG, 40 μm for LOP01
Carrier gas flow rate		MFC1: 1.9 L min^{-1} (He), MFC2: 1.9 L min^{-1} (He)
Pulse rate		12 Hz

Table 2 Faraday cup configuration of Neptune and Neptune Plus for Sr–Nd–Hf isotopic measurement

Cup	L4	L3	L2	L1	C	H1	H2	H3	H4
Neptune									
Sr[a]	^{83}Kr	83.5	^{84}Sr	^{85}Rb	^{86}Sr	86.5	^{87}Sr	^{88}Sr	^{89}Y
Nd[b]	^{142}Nd	^{143}Nd	^{144}Nd	^{145}Nd	^{146}Nd	^{147}Sm	^{149}Sm	^{150}Nd	^{154}Sm
Neptune Plus									
Nd[a]	^{142}Nd	^{143}Nd	^{144}Nd	^{145}Nd	^{146}Nd	^{147}Sm	^{149}Sm	^{150}Nd	^{154}Sm
Hf[b]	^{172}Yb	^{173}Yb	^{175}Lu	^{176}Hf	^{177}Hf	^{178}Hf	^{179}Hf	^{180}Hf	^{182}W

[a] Denotes simultaneous measurement of Sr–Nd isotope. [b] Denotes simultaneous measurement of Nd–Hf isotope.

exponential law. Finally, the $^{87}Sr/^{86}Sr$, $^{87}Rb/^{86}Sr$, $^{84}Sr/^{86}Sr$ and $^{84}Sr/^{88}Sr$ ratios were normalized using the exponential law.[4,5,12]

For Nd isotopic analysis, the isobaric interference of ^{144}Sm on ^{144}Nd is significant. We used the measured $^{147}Sm/^{149}Sm$ ratio to calculate the Sm fractionation factor and the measured ^{147}Sm intensity using the natural $^{147}Sm/^{144}Sm$ ratio to estimate the Sm interference on mass 144. The interference-corrected $^{146}Nd/^{144}Nd$ ratio can then be used to calculate the Nd fractionation factor. Finally, the $^{147}Sm/^{144}Nd$, $^{143}Nd/^{144}Nd$ and $^{145}Nd/^{144}Nd$ ratios were normalized using the exponential law.[12,18]

For Hf isotopic analysis, the isobaric interference of ^{176}Lu on ^{176}Hf is negligible due to the low $^{176}Lu/^{177}Hf$ in the zirconolite (normally <0.0002) and eudialyte (normally <0.001). In this study, $^{176}Lu/^{175}Lu = 0.02655$ was used to extract the interference of ^{176}Lu on ^{176}Hf. However, the interference of ^{176}Yb on ^{176}Hf must be carefully corrected since the contribution of ^{176}Yb to ^{176}Hf could profoundly affect the accuracy of the measured $^{176}Hf/^{177}Hf$ ratio. During analysis, an isotopic ratio of $^{176}Yb/^{172}Yb = 0.588673$ was applied. Finally, the $^{176}Yb/^{177}Hf$, $^{176}Lu/^{177}Hf$, $^{176}Hf/^{177}Hf$ ratios were normalized using the exponential law given in the ref. 10.

2.3. Investigation for simultaneous determination

Because of the different concentrations of Sr, Nd and Hf in the analyzed minerals, the proportions of ablated aerosol carried into the Neptune and Neptune Plus MC-ICP-MSs were adjusted to obtain precise data for Sr, Nd and Hf isotopic compositions. In this case, the main question is whether there is any mass fractionation when different proportions of ablated material are simultaneously carried into the Neptune and Neptune Plus MC-ICP-MSs. In this study, our *in-house* reference materials for apatite (SDG) and loparite (LOP01) were used to answer the above question. The SDG apatite was obtained from the Sandaogou alkaline ultramafic complex in Inner Mongolia, China,[20] and the LOP01 loparite was obtained from the eudialyte lujavrites layered intrusion from the western part of the complex between the Alluaiv and Punkaruaiv Mountains, Greenland.[21]

The SDG apatite was ablated using an analyte G2 laser ablation system, with 12 Hz frequency and 50 μm spot size. Three different proportions (3 : 7, 5 : 5 and 7 : 3) of ablated materials were split into two MC-ICP-MSs (Neptune and Neptune Plus) for the measurement of Sr and Nd isotopic compositions. The obtained mean $^{87}Sr/^{86}Sr$ ratios of SDG apatite by Neptune were 0.70302 ± 11 (2SD, $n = 10$, [3 : 7]) (Fig. 2a), 0.70301 ± 04 (2SD, $n = 10$, [5 : 5]) (Fig. 2c) and 0.70304

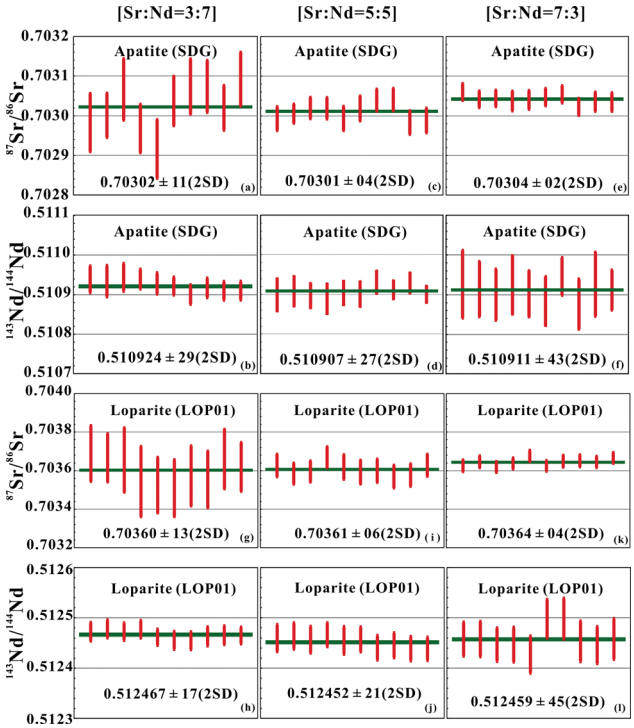

Fig. 2 $^{87}Sr/^{86}Sr$ and $^{143}Nd/^{144}Nd$ ratio of the simultaneous *in situ* Sr–Nd isotope analyses for SDG apatite and LOP01 loparite measured using different gas ratios. For SDG, the gas stream (Sr) : the gas stream (Nd) = 3 : 7 (a and b), the gas stream (Sr) : the gas stream (Nd) = 5 : 5 (c and d), and the gas stream (Sr) : the gas stream (Nd) = 7 : 3 (e and f). For LOP01, the gas stream (Sr) : the gas stream (Nd) = 3 : 7 (g and h), the gas stream (Sr) : the gas stream (Nd) = 5 : 5 (i and j), and the gas stream (Sr) : the gas stream (Nd) = 7 : 3 (k and l).

± 02 (2SD, $n = 10$, [7 : 3]) (Fig. 2e); whereas, the obtained mean $^{143}Nd/^{144}Nd$ ratios by the Neptune Plus were 0.510924 ± 29 (2SD, $n = 10$, [3 : 7]) (Fig. 2b), 0.510907 ± 27 (2SD, $n = 10$, [5 : 5]) (Fig. 2d) and 0.510911 ± 43 (2SD, $n = 10$, [7 : 3]) (Fig. 2f) (see ESI Table 1†). The achieved $^{87}Sr/^{86}Sr$ ratios are in agreement within analytical errors and are the same as the reference value of 0.70300 ± 01 (2SD, $n = 5$) obtained by the solution method.[12] The $^{143}Nd/^{144}Nd$ ratios are also identical within analytical errors with the reference value of 0.510918 ± 14 (2SD, $n = 5$) obtained by the solution method.[12]

The same analytical procedure was used to measure the Sr and Nd isotopic compositions of loparite (LOP01), with a spot size of 40 μm. The mean $^{87}Sr/^{86}Sr$ ratios of LOP01 measured by the Neptune were as follows: 0.70360 ± 13 (2SD, $n = 10$, [3 : 7]) (Fig. 2g), 0.70361 ± 06 (2SD, $n = 10$, [5 : 5]) (Fig. 2i); and 0.70364 ± 04 (2SD, $n = 10$, [7 : 3]) (Fig. 2k). They are consistent within analytical errors and are identical to the reference value of 0.70362 ± 04 (2SD, $n = 3$) measured by TIMS.[21] The mean $^{143}Nd/^{144}Nd$ ratios obtained by the Neptune Plus were 0.512467 ± 17 (2SD, $n = 10$, [3 : 7]) (Fig. 2h), 0.512452 ± 21 (2SD, $n = 10$, [5 : 5]) (Fig. 2j) and 0.512459 ± 45 (2SD, $n = 10$, [7 : 3]) (Fig. 2l) (see ESI Table 2†). They are identical within analytical errors and are the same as the reported value of 0.512468 ± 18 (2SD, $n = 5$) obtained by the TIMS method.[21] Therefore, we concluded that there was no significant mass fractionation when different proportions of ablated material were carried into the Neptune and the Neptune Plus MC-ICP-MSs.

3. Results

3.1. Sr–Nd simultaneous measurement

We first present our *in situ* simultaneous Sr–Nd isotopic analyses (Sr measured in the Neptune and Nd in the Neptune Plus) for apatite, loparite, eudialyte and perovskite (see ESI Table 3†).

3.1.1. Apatite. AP1 is an *in-house* apatite reference material, which is probably from Madagascar.[12] ID-TIMS analysis for this apatite standard gave a weighed mean $^{206}Pb/^{238}U$ age of 475 Ma.[22] The $^{87}Sr/^{86}Sr$ isotopic data are shown in Fig. 3a, yielding a mean $^{87}Sr/^{86}Sr$ ratio of 0.71137 ± 14 (2SD, $n = 10$). The mean value is identical to the reported solution value of 0.71137 ± 03 (2SD, $n = 14$) within analytical errors.[12] The results show that the obtained $^{143}Nd/^{144}Nd$ ratio of AP1 apatite is 0.511348 ± 47 (2SD, $n = 10$) (Fig. 3b), which is consistent with the published value of 0.511352 ± 24 (2SD, $n = 12$).[12] The corresponding $\varepsilon_{Nd}(t)$ value of −18.2 ± 0.90 (2SD, $n = 10$) is almost identical to the $\varepsilon_{Nd}(t)$ value of −18.2 ± 0.50 (2SD, $n = 10$) obtained by the solution method.[12]

MAD apatite is an international reference material from the 1st Mine Discovery in Madagascar,[12] with a TIMS U–Pb age of 485.2 ± 0.8 Ma.[22,23] The simultaneous *in situ* $^{87}Sr/^{86}Sr$ and $^{143}Nd/^{144}Nd$ isotopic data are shown in Fig. 3c and d. The results show that the mean $^{87}Sr/^{86}Sr$ ratio of MAD apatite is 0.71190 ± 10 (2SD, $n = 10$) (Fig. 3c), which is identical to the solution mean value of 0.71180 ± 03 (2SD, $n = 11$)[12] within analytical errors. The $^{143}Nd/^{144}Nd$ result of the MAD apatite is 0.511346 ± 31 (2SD, $n = 10$) (Fig. 3d), which is consistent with the published

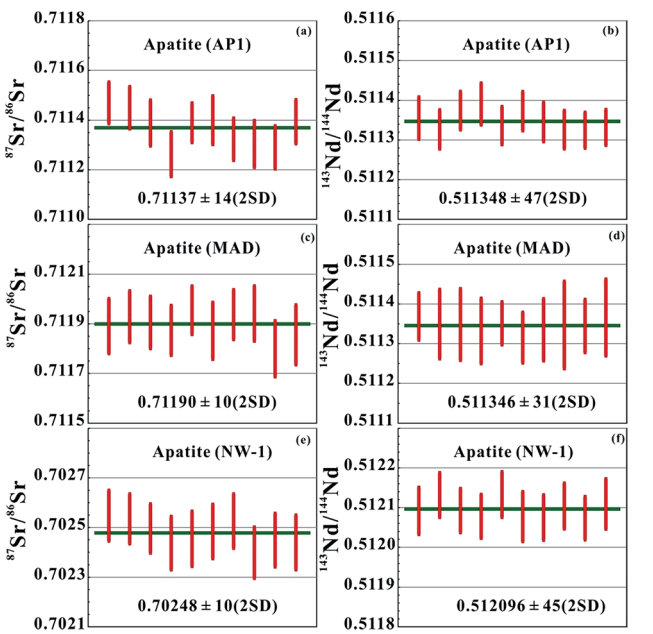

Fig. 3 $^{87}Sr/^{86}Sr$ and $^{143}Nd/^{144}Nd$ ratio of the simultaneous *in situ* Sr–Nd isotope analyses for AP1 apatite (a and b), MAD apatite (c and d) and NW-1 apatite (e and f).

value of 0.511348 ± 16 (2SD, $n = 5$).[12] The corresponding $\varepsilon_{Nd}(t)$ of −18.1 ± 0.7 (2SD, $n = 10$) is almost identical to the $\varepsilon_{Nd}(t)$ value of −18.1 ± 0.3 (2SD, $n = 5$), obtained by the solution method.[12]

NW-1 apatite is from a carbonatite in the Prairie Lake alkaline carbonatite complex in Ontario, Canada[6–8,22,24,25] with a U–Th–Pb age of 1160 ± 5 Ma, measured by SIMS.[25] Our results show that the mean $^{87}Sr/^{86}Sr$ ratio of NW-1 apatite is 0.70248 ± 10 (2SD, $n = 10$) (Fig. 3e), which is identical to the solution mean value of 0.70250 ± 02 (2SD, $n = 11$)[12] within analytical errors. The $^{143}Nd/^{144}Nd$ ratio of the NW-1 apatite is 0.512096 ± 45 (2SD, $n = 10$) (Fig. 3f), which is consistent with the published value of 0.512104 ± 11 (2SD, $n = 7$).[12] The corresponding $\varepsilon_{Nd}(t)$ value of 3.58 ± 0.85 (2SD, $n = 10$) is almost identical to the value of 3.77 ± 0.14 (2SD, $n = 7$), obtained by the solution method.[12]

3.1.2. Perovskite. The AFK perovskite standard was extracted from an irregular pegmatite body collected from the Afrikanda complex in the Kola Peninsula, Russia.[26] The TIMS analyses yielded a weighed mean $^{206}Pb/^{238}U$ age of 382 ± 1 Ma.[26] Our results indicate a mean $^{87}Sr/^{86}Sr$ of 0.70340 ± 08 (2SD, $n = 10$) (Fig. 4a), which is similar to the TIMS mean value of 0.70335 ± 04 (2SD, $n = 5$)[26] within analytical errors. The $^{143}Nd/^{144}Nd$ ratio of this standard is 0.512610 ± 49 (2SD, $n = 10$) (Fig. 4b), which is consistent with the published value of 0.512609 ± 27 (2SD, $n = 3$).[26] The corresponding $\varepsilon_{Nd}(t)$ value of 5.88 ± 0.86 (2SD, $n = 10$) is almost identical to the value of 5.83 ± 0.58 (2SD, $n = 3$), obtained by the solution method.[26]

3.1.3. Loparite. Kramm and Kogarko[27] reported a whole rock Rb–Sr isochron age for the Lovozero and Khibiny (Kola Peninsula, Russia) loparite standard of 370.4 ± 6.7 Ma. Our results show that the mean $^{87}Sr/^{86}Sr$ ratio is 0.70361 ± 11 (2SD, $n = 10$), which is consistent with the TIMS mean value of 0.70362 ± 04 (2SD, $n = 3$) within analytical errors (Fig. 4c).[21] The $^{143}Nd/^{144}Nd$ ratio of this standard is 0.512463 ± 71 (2SD, $n = 10$) (Fig. 4d), which is identical to the published value of 0.512468 ± 18 (2SD, $n = 5$).[21] The corresponding $\varepsilon_{Nd}(t)$ of 4.05 ± 1.39 (2SD, $n = 10$) is similar to the $\varepsilon_{Nd}(t)$ value of 3.72 ± 0.70 (2SD, $n = 5$) obtained by the solution method.[21]

3.1.4. Eudialyte. The LV01 eudialyte standard comes from a pegmatitic syenite occurring in the Lovozero alkaline complex (Kola Peninsula, Russia). The LA-ICP-MS analyses yielded a weighted mean $^{206}Pb/^{238}U$ age of 376 ± 6 Ma.[6] The mean $^{87}Sr/^{86}Sr$ ratio is 0.70399 ± 05 (2SD, $n = 10$) (Fig. 4e), which is the same as the reported TIMS mean value of 0.70392 ± 02 (2SD, $n = 3$)[6] within analytical errors. The $^{143}Nd/^{144}Nd$ ratio for this standard is 0.512641 ± 43 (2SD, $n = 10$) (Fig. 4f), which is consistent with the published value of 0.512702 ± 28 (2SD, $n = 2$).[6] The corresponding $\varepsilon_{Nd}(t)$ of 3.89 ± 0.82 (2SD, $n = 10$) is almost identical to the $\varepsilon_{Nd}(t)$ value of 4.94 ± 0.62 (2SD, $n = 2$), obtained by the solution method.[6]

3.2. Nd–Hf simultaneous measurement

We conducted *in situ* simultaneous Nd–Hf isotopic analyses (Nd measured in the Neptune and Hf measured in the Neptune Plus) for eudialyte and zirconolite (see ESI Table 4†).

3.2.1. Eudialyte. As shown in Fig. 5a, twelve analyses of LV01 eudialyte standard yield a mean $^{143}Nd/^{144}Nd$ ratio of 0.512658 ± 66 (2SD), which is consistent with the published value of 0.512702 ± 28 (2SD, $n = 2$).[6] The corresponding $\varepsilon_{Nd}(t)$ value is 4.20 ± 1.25 (2SD, $n = 12$), which is similar with the errors of the solution TIMS method value of 4.94 ± 0.62 (2SD, $n = 2$).[6] Moreover, as displayed in Fig. 5b, the twelve analyses of LV01 eudialyte give a mean $^{176}Hf/^{177}Hf$ ratio of 0.282806 ± 57 (2SD), which is well within the error of the reported TIMS mean value of 0.282761 ± 18 (2SD, $n = 5$).[6] The corresponding $\varepsilon_{Hf}(t)$ of 8.79 ± 1.99 (2SD, $n = 12$) is similar to the $\varepsilon_{Hf}(t)$ value of 7.08 ± 0.66 (2SD, $n = 5$), obtained by the solution method.[6]

3.2.2. Zirconolite. The ZrkA zirconolite standard was collected in the Phalaborwa Mine, Loolekop complex (Gauteng

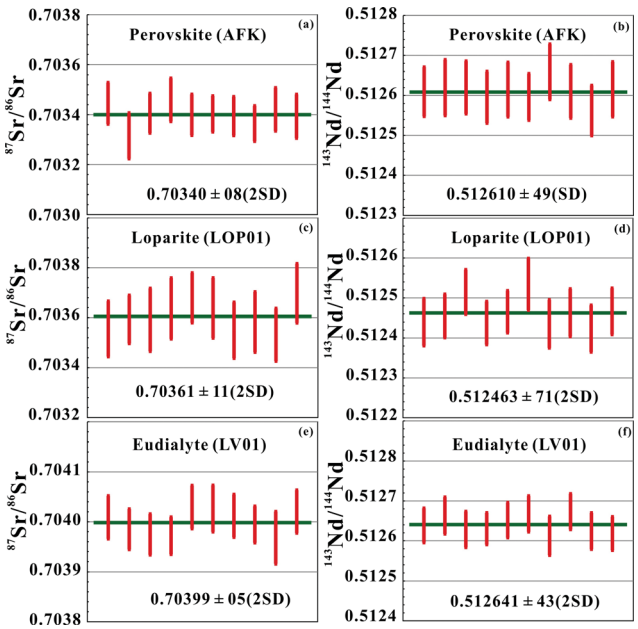

Fig. 4 $^{87}Sr/^{86}Sr$ and $^{143}Nd/^{144}Nd$ ratio of the simultaneous *in situ* Sr–Nd isotope analyses for AFK perovskite (a and b), LOP01 Loparite (c and d) and LV01 eudialyte (e and f).

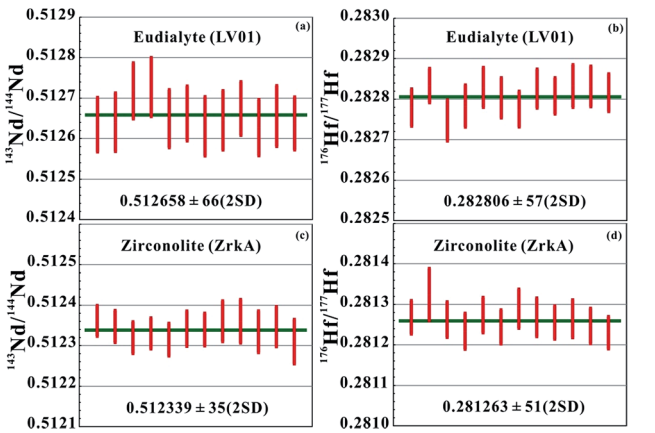

Fig. 5 $^{143}Nd/^{144}Nd$ and $^{176}Hf/^{177}Hf$ ratio of the simultaneous *in situ* Nd–Hf isotope analyses for LV01 eudialyte (a and b) and ZrkA zirconolite (c and d).

province, Republic of South Africa), and it consists of a single prismatic crystal lacking any matrix. The reported age of this standard is ~2060 Ma on SIMS Pb–Pb.[7] The measured Nd isotopic data is displayed in Fig. 5c with a mean $^{143}Nd/^{144}Nd$ ratio of 0.512339 ± 35 (2SD, $n = 12$), which is consistent with the published value of 0.512323 ± 08 (2SD, $n = 5$).[7] The corresponding $\varepsilon_{Nd}(t)$ value is −6.47 ± 1.26 (2SD, $n = 12$), which is similar within the uncertainty of the solution TIMS value of −5.60 ± 0.20 (2SD, $n = 5$).[7] The Hf isotopic analysis measured in this study gives a mean $^{176}Hf/^{177}Hf$ ratio of 0.281263 ± 51 (2SD, $n = 12$) (Fig. 5d), which is well within the error of the reported solution mean value of 0.281296 ± 05 (2SD, $n = 5$).[7] The corresponding $\varepsilon_{Hf}(t)$ of −8.03 ± 1.79 (2SD, $n = 12$) is almost identical to the $\varepsilon_{Hf}(t)$ value of −6.80 ± 0.20 (2SD, $n = 5$), obtained by the solution method.[7]

4. Discussion

Natural minerals usually have complex crystal structures, *i.e.*, fine-scale zoning as well as growth zoning. Such growth zones can be distinct both in composition and age on a single grain or sub-grain scale.[17,28] Therefore, it is better for researchers to conduct *in situ* analysis in either a thin section or grain epoxy mounts with a spatial resolution to suit the problem being addressed.[16,29,30] Previous *in situ* Sr, Nd and Hf isotopic measurements on different minerals were conducted for more than one ablation event using different volumes of ablated materials, which increases the level of sampling uncertainty because of the discrimination in the ablation volumes, depths and locations.[17] Considering the widely used Sr–Nd (*e.g.*, $[^{87}Sr/^{86}Sr]_i - \varepsilon_{Nd}t$) or Nd–Hf (*e.g.*, $\varepsilon_{Nd}t - \varepsilon_{Hf}t$) diagrams to trace the petrogenesis and evolution of the Earth, our *in situ* simultaneous Sr–Nd or Nd–Hf isotopic analysis of the same volume of material brings an ideal solution to the sampling limitations mentioned above.

In contrast to previous analytical techniques of different ablated material in different analytical sessions, our developed method maximizes the amount of useful isotopic data that can be obtained from a single spot analysis using two MC-ICP-MSs. This technique is very suitable for natural minerals with enriched Sr and Nd contents, such as apatite, perovskite, loparite and eudialyte,[6,12,21,26] and those with relatively enriched Nd and Hf concentrations, *i.e.*, zirconolite and eudialyte.[7,26] Furthermore, as shown in ESI Tables 3 and 4,† the precision and accuracy of Sr, Nd and Hf isotope data, measured using our developed methodology were assessed and evaluated by five natural minerals from the reference materials in the collection in our laboratory, demonstrating the applicability and robustness of our developed approach.

Nevertheless, the main limitation of simultaneous measurement is that the signal strength on each MC-ICP-MS decreases when compared to the separate measurements of Sr, Nd or Hf isotopes. This drawback happens because the total volume of ablated material is split into two MC-ICP-MS instruments. The tables in the ESI† provide more information on the extent of the loss of signal intensity. In addition, not all minerals can be simultaneously measured using our method due to their lower element concentrations and potential interferences. Only the minerals with high concentrations of Sr, Nd and Hf can be used for the simultaneous determination of Sr, Nd and Hf isotopic compositions with reasonable analytical precision (*e.g.*, eudialyte). According to our study, more than 1000 ppm of Sr is enough to yield data with a precision of ±0.0001 if a large spot size is used (ESI Table 3†). For Nd isotopic analysis, the deviation requirement for practical geological application is $\pm 2\varepsilon$ units, corresponding to a $^{143}Nd/^{144}Nd$ data deviation of ±0.0001.[6–8] More than ~1000 ppm of Nd is enough for most Nd enriched accessory minerals. As for simultaneous Nd–Hf isotopic measurement, only a few minerals (*e.g.*, eudialyte and zirconolite) are feasible if they contain relatively high concentrations of Nd and Hf (ESI Table 4†).

5. Conclusion

We present an analytical protocol for using laser ablation (Analyte G2) together with two MC-ICP-MSs to measure Sr–Nd or Nd–Hf isotopes simultaneously for a single ablation event. There are insignificant variations in the Sr, Nd and Hf isotopic ratios when the different proportions of ablated material are carried into the Neptune and Neptune Plus MC-ICP-MSs, indicating that there is no evident elemental (or isotopic) fractionation during the transportation of the laser ablation aerosol. Sr, Nd and Hf isotopic values for eight samples of five natural minerals obtained by this method are identical to the reference values within analytical errors, indicating the feasibility of using the proposed method. Our technique is of value in applications requiring Sr, Nd and Hf isotopic compositions from a single sampling site, which provides a powerful tool for the petrogenetic studies related to the geological evolution of our planet.

Acknowledgements

This study was financially supported by the Natural Science Foundation of China (NSFC Grants 41221002, 41403002, 41473012 and 41273021). We are greatly indebted to Dr Yamirka Rojas-Agramonte for correcting the English during our submission and revision. We are also grateful to two anonymous reviewers for critical and insightful comments that greatly improved this manuscript.

References

1 P. D. Kinny and R. Maas, *Rev. Mineral. Geochem.*, 2003, **53**, 327–341.
2 T. M. Harrison, J. Blichert-Toft, W. Muller, F. Albarede, P. Holden and S. J. Mojzsis, *Science*, 2005, **310**, 1947–1950.
3 C. J. Hawkesworth and A. I. S. Kemp, *Chem. Geol.*, 2006, **226**, 144–162.
4 Y. H. Yang, F. Y. Wu, S. A. Wilde, X. M. Liu, Y. B. Zhang, L. W. Xie and J. H. Yang, *Chem. Geol.*, 2009, **264**, 24–42.
5 Y. H. Yang, F. Y. Wu, L. W. Xie, J. H. Yang and Y. B. Zhang, *Acta Pet. Sin.*, 2009, **25**, 3431–3441.

6 F. Y. Wu, Y. H. Yang, M. A. W. Marks, Z. C. Liu, Q. Zhou, W. C. Ge, J. S. Yang, Z. F. Zhao, R. H. Mitchell and G. Markl, *Chem. Geol.*, 2010, **273**, 8–34.
7 F. Y. Wu, Y. H. Yang, R. H. Mitchell, F. Bellatreccia, Q. L. Li and Z. F. Zhao, *Chem. Geol.*, 2010, **277**, 178–195.
8 F. Y. Wu, Y. H. Yang, R. H. Mitchell, Q. L. Li, J. H. Yang and Y. B. Zhang, *Lithos*, 2010, **115**, 205–222.
9 G. L. Foster and D. Vance, *J. Anal. At. Spectrom.*, 2006, **21**, 288–296.
10 F. Y. Wu, Y. H. Yang, L. W. Xie, J. H. Yang and P. Xu, *Chem. Geol.*, 2006, **234**, 105–126.
11 C. R. M. McFarlane and M. T. McCulloch, *Chem. Geol.*, 2007, **245**, 45–60.
12 Y. H. Yang, F. Y. Wu, J. H. Yang, D. M. Chew, L. W. Xie, Z. Y. Chu, Y. B. Zhang and C. Huang, *Chem. Geol.*, 2014, **385**, 35–55.
13 L. Xu, Z. Hu, W. Zhang, L. Yang, Y. Liu, S. Gao, T. Luo and S. Hu, *J. Anal. At. Spectrom.*, 2015, **30**, 232–244.
14 L. W. Xie, Y. B. Zhang, H. H. Zhang, J. F. Sun and F. Y. Wu, *Chin. Sci. Bull.*, 2008, **53**, 1565–1573.
15 H. L. Yuan, S. Gao, M. N. Dai, C. L. Zong, D. Gunther, G. H. Fontaine, X. M. Liu and C. Diwu, *Chem. Geol.*, 2008, **247**, 100–118.
16 D. L. Tollstrup, L. W. Xie, J. B. Wimpenny, E. Chin, C. T. Lee and Q. Z. Yin, *Geochem., Geophys., Geosyst.*, 2012, **13**, Q03017.
17 D. J. Goudie, C. M. Fisher, J. M. Hanchar, J. L. Crowley and J. C. Ayers, *Geochem., Geophys., Geosyst.*, 2014, **15**, 2575–2600.
18 Y. H. Yang, J. F. Sun, L. W. Xie, H. R. Fan and F. Y. Wu, *Chin. Sci. Bull.*, 2008, **53**, 1062–1070.
19 Y. H. Yang, F. Y. Wu, L. W. Xie, Z. Y. Chu and J. H. Yang, *Spectrochim. Acta, Part B*, 2014, **97**, 118–123.
20 H. Y. Zhou, J. Z. Geng, Y. R. Cui and H. M. Li, *Acta Geol. Sin.*, 2012, **33**, 857–864, in Chinese with English abstract.
21 R. H. Mitchell, F. Y. Wu and Y. H. Yang, *Chem. Geol.*, 2011, **280**, 191–199.
22 Q. Zhou, Ph. D., University of Chinese Academy of Sciences and Institute of Geology and Geophysics, Chinese Academy of Science, doctoral dissertation, 2013, in Chinese with English abstract.
23 S. N. Thomson, G. E. Gehrels, J. Ruiz and R. Buchwaldt, *Geochem., Geophys., Geosyst.*, 2012, **13**, Q0AA21.
24 Y. Sano, T. Oyama, K. Terada and H. Hidaka, *Chem. Geol.*, 1999, **153**, 249–258.
25 Q. L. Li, X. H. Li, F. Y. Wu, Q. Z. Yin, H. M. Ye, Y. Liu, G. Q. Tang and C. L. Zhang, *Gondwana Res.*, 2012, **21**, 745–756.
26 F. Y. Wu, A. A. Arzamastsev, R. H. Mitchell, Q. L. Li, J. Sun, Y. H. Yang and R. C. Wang, *Chem. Geol.*, 2013, **353**, 210–229.
27 U. Kramm and L. N. Kogarko, *Lithos*, 1994, **32**, 225–242.
28 M. J. Kohn and J. D. Vervoort, *Geochem., Geophys., Geosyst.*, 2008, **9**, Q04031.
29 Z. C. Liu, F. Y. Wu, Y. H. Yang, J. H. Yang and S. A. Wilde, *Chem. Geol.*, 2012, **334**, 221–239.
30 M. L. Williams and M. J. Jercinovic, *J. Metamorph. Geol.*, 2012, **30**, 739–752.